

Subscriber access provided by TULANE UNIV

Article

C#D Modes of Deuterated Side Chain of Leucine as Structural Reporters via Dual-frequency Two-dimensional Infrared Spectroscopy

Sri Ram G. Naraharisetty, Valeriy M. Kasyanenko, Jo#rg Zimmermann, Megan C. Thielges, Floyd E. Romesberg, and Igor V. Rubtsov

J. Phys. Chem. B, 2009, 113 (14), 4940-4946 DOI: 10.1021/jp8112446 Publication Date (Web): 19 March 2009

Downloaded from http://pubs.acs.org on April 27, 2009

More About This Article

Additional resources and features associated with this article are available within the HTML version:

- Supporting Information
- Access to high resolution figures
- Links to articles and content related to this article
- Copyright permission to reproduce figures and/or text from this article

View the Full Text HTML



C-D Modes of Deuterated Side Chain of Leucine as Structural Reporters via Dual-frequency Two-dimensional Infrared Spectroscopy

Sri Ram G. Naraharisetty,[†] Valeriy M. Kasyanenko,[†] Jörg Zimmermann,[‡] Megan C. Thielges,[‡] Floyd E. Romesberg,[‡] and Igor V. Rubtsov*,[†]

Department of Chemistry, Tulane University, New Orleans, Louisiana 70118 and Department of Chemistry, The Scripps Research Institute, La Jolla, California 92037

Received: December 19, 2008; Revised Manuscript Received: February 3, 2009

Perdeuteration of the side chains of amino acids such as leucine results in appearance of reasonably strong absorption peaks around $2050-2220 \text{ cm}^{-1}$ that belong to the CD stretching modes and exhibit extinction coefficients of up to $120 \text{ M}^{-1} \text{ cm}^{-1}$. The properties of the CD stretching transitions in leucine- d_{10} as structural labels are studied via the methods of two-dimensional infrared (2DIR) spectroscopy. The cross peaks caused by interactions of the CD stretching modes with amide I (Am–I), CO, and amide II (Am–II) modes are obtained by the dual-frequency 2DIR method. The CD stretching peaks in leucine- d_{10} are characterized using DFT computational modeling as well as relaxation-assisted 2DIR (RA 2DIR) measurements. The RA 2DIR measurements showed different enhancements and different energy transport times (arrival times) for different CD/Am–II and CD/CO cross peaks; a correlation between the intermode distance, the arrival time, and the amplification factor is reported. We demonstrated that the CD transitions of leucine- d_{10} amino acid can serve as convenient structural reporters via the dual-frequency 2DIR methods and discussed the potential of leucine- d_{10} and other amino acids with deuterium-labeled side chains as probes of protein structure and dynamics.

1. Introduction

Development of approaches for accurately probing threedimensional (3D) structures and dynamics of structural changes of large biological molecules under physiological conditions is important for understanding the physical basis of molecular recognition and catalysis. Two-dimensional infrared spectroscopy (2DIR) has emerged as a powerful technique for obtaining structural constraints for molecules in solution at a variety of temperatures, 1,2 as it is capable of monitoring structural distributions with the averaging time window in the range of several tens of picoseconds 3-12 and is also capable of measuring dynamics of structural changes on a wide range of time scales from subpicoseconds^{13–16} to seconds,^{17–20} hours,²¹ and days.²² 2DIR spectroscopy permits accessing the distances between vibrating groups and the angles between transition moments of the respective vibrational modes by measuring the cross peaks between interacting modes.²³ The dual-frequency 2DIR technique (DF 2DIR), 24-27 which is similar to the heteronuclear 2D NMR method, ²⁸ is able to characterize the interactions between vibrational modes with very different vibrational frequencies, to eliminate diagonal peaks, and focus solely on the cross peaks that are most useful for delivering structural constraints.

The application of 2DIR to biological molecules such as proteins holds the potential to dramatically extend our ability to characterize their structure and dynamics. However, this requires the introduction of single or multiple nonperturbative labels with vibrational transitions that are distinct from the other transitions in the molecule and/or solvent. Several labeling strategies have been tested, including isotope labeling $^{22,29-33}$ and utilization of weak modes, such as $C \equiv N$, 26,34,35 SH, 36 and SO³⁷

stretches, as well as modes in the fingerprint region of the IR spectrum (900–1500 cm⁻¹). ³⁸ For example, ¹³C=¹⁸O isotope substitution shifts the amide I (Am–I) frequency by ca. 65 cm⁻¹, thereby spectrally isolating the labeled mode from the rest of the Am–I modes. Although such labeling has been shown to work well for a number of peptides of up to about 40 amino acids, ³⁹ the 65 cm⁻¹ shift might not be large enough to spectrally isolate the mode in large proteins due to the large width of the Am–I band and the presence of other protein modes of commensurate frequencies.

In contrast, carbon—deuterium (C–D) bonds absorb in an otherwise transparent region of the proteins IR spectrum. Indeed, C–D labels have been site-selectively incorporated into the proteins cytochrome c^{40-46} and dihydrofolate reductase⁴⁷ and are used to provide high structural and temporal resolution of folding and/or dynamics. Although the use of CD probes in linear IR^{41,48-51} and 2DIR^{10,33,52,53} spectroscopies is challenging due to their relatively small extinction coefficients, this did not prevent the observation of cross peaks between the CD and CN modes in the small molecule acetonitrile- d_3 , where the extinction coefficient of the symmetric CD₃ stretching mode is ca. 1 M⁻¹ cm^{-1,33} or between the CD and CO modes in formamide- d_3^{52} and in benzaldehyde- d_6 .⁵⁴

In all reported 2DIR studies involving CD labels, the two modes probed, CD and CN,³³ CD and CO,^{52,54} or CD and CC,⁵⁴ were largely spatially overlapping, that is, the same or adjacent atoms are engaged in motion when the modes are excited, which resulted in substantial anharmonic coupling and increased the cross-peak amplitude. As the distance between the probed modes increases, the anharmonic coupling (direct coupling) decreases rapidly,²⁷ which may render CD labels inefficient for the 2DIR measurements over larger distances. The recently proposed relaxation-assisted 2DIR spectroscopy (RA 2DIR) method permits enhancing the cross peaks between spatially remote modes utilizing energy relaxation and energy transport phe-

 $[\]mbox{\ensuremath{\ast}}$ To whom correspondence should be addressed. E-mail: irubtsov@ tulane.edu.

[†] Tulane University.

^{*} The Scripps Research Institute.

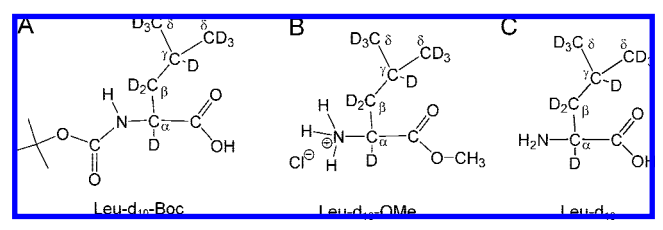


Figure 1. Structure of (A) Leu- d_{10} -Boc; (B) Leu- d_{10} -OMe (methyl ester hydrochloride); and (C) Leu- d_{10} amino acid.

nomena.²⁷ An 18-fold amplification of the cross peak amplitude between C≡N and C=O stretching modes separated by ca. 11 Å has been reported using the RA 2DIR method.³⁸ In this example, vibrational modes at the C=O group site are excited via energy transport from the initially excited C≡N mode. Spatial overlap of the modes with the C=O mode ensures their strong coupling and causes the cross-peak amplification. Note that the probability of exciting the C=O mode via energy transport from the C≡N mode is small due to its high frequency, large distance between the CN and CO groups, and large density of states in the molecule. It has also been shown that the energy transport time (the arrival time) between the sites where the two modes are located is correlated with the distance between the sites, providing an additional, easily accessible, parameter that can be linked to the molecular structure. Due to the crosspeak enhancement, the RA 2DIR approach permits the use of weak IR modes as structural reporters for substantially larger separation distances.

As part of an effort to utilize C-D bonds and 2DIR spectroscopy for the characterization of protein structure and dynamics, we investigated properties of the C-D transitions of a perdeuterated leucine side chain. Perdeuteration of the side chain of leucine amino acid (Leu- d_{10}) has been shown to result in a CD stretching transition at ca. 2220 cm^{-1 47} with an extinction coefficient of ca. 120 M⁻¹ cm⁻¹ (Figure 2). In this work we investigated properties of the CD transitions of leucine d_{10} and tested the potential of such CD labels as structural reporters via 2DIR spectroscopy. We measured the direct coupling of the CD transitions with amide II (Am-II) and C=O modes in leucine- d_{10} , assigned the CD transitions, and tested the energy transport properties of the side chain using the RA 2DIR method.

2. Experimental Methods

2.1. Dual-frequency 2DIR and Relaxation-assisted 2DIR **Measurements.** The fundamental laser pulses at 806 nm with 44 fs duration were produced by a Ti:sapphire-oscillator/ regenerative amplifier tandem (Vitasse/USP-Legend, Coherent). The fundamental pulses were used to pump two in-house-built optical parametric amplifiers (OPA). Each OPA generates a pair of near-IR pulses, signal and idler, that are used to generate a pair of independently tunable mid-IR pulses via a differencefrequency-generation process in a 1.5 mm thick AgGaS₂ crystal (see details of the setup in ref 26). The spectral width of the mid-IR pulses was $175 \pm 10 \text{ cm}^{-1}$. Each mid-IR beam was split into two parts; three pulses were focused onto the sample and the fourth was used as a local oscillator (LO) for the heterodyned detection. The third-order signal generated in the sample was picked in the phase matching direction $(-k_1 + k_2)$ $+ k_3$), and mixed with LO at the MCT detector. The time delays between the first and the second pulses and the second and the third pulses are referred to as the dephasing time, τ , and the

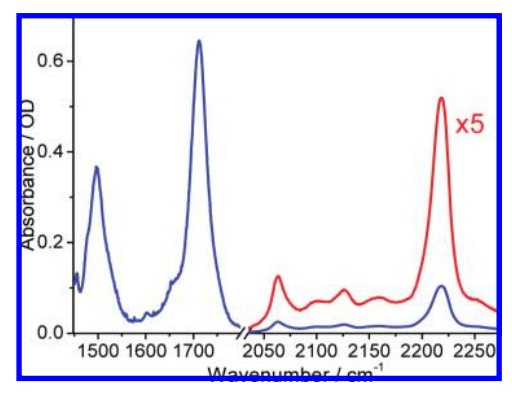


Figure 2. FTIR spectrum of Leu- d_{10} -Boc in chloroform.

waiting time, T, respectively. The delay of the LO with respect to the third pulse is referred to as the detection time, t.

For the cross peak measurements between the modes at ω_1 and ω_2 frequencies, the spectra of the $(k_1$ and $k_2)$ and (k_3) and LO) pulses were tuned to center at ω_1 and ω_2 , respectively. The dual-frequency phase-matching conditions were satisfied by setting up the pulse geometry at the sample such that the k_1 , k_2 , and k_3 pulses are directed toward the corners of the trapeze having the ratio of the base lengths equal to the ratio of the ω_1/ω_2 (k_1/k_3) frequencies so that the higher frequency, here k_1 and k_2 pulses, hit the corners of the smaller base of the trapeze. 26,33 Two-dimensional (t, τ) data sets were recorded keeping the waiting time, T, fixed and double-Fourier transformed to obtain the (ω_t, ω_τ) 2DIR spectrum. Several 2DIR (ω_t, ω_τ) spectra were measured at different waiting times, T, to demonstrate the evolution of the cross peaks with the waiting time, T. The polarizations of the mid-IR pulses were set by the pairs of a zero-order waveplate and a polarizer.

To accelerate the measurements of the cross-peak amplitude as a function of T, a set of single scans along the dephasing time, τ , at different waiting times, T, was recorded keeping the detection time, t, constant. The (τ, T) data sets were then Fourier transformed along the τ direction and presented as a set of one-dimensional (1D) ω_{τ} spectra at various T values. Note, that the peak in the ω_{τ} spectrum have contributions from all the peaks seen at the same ω_t frequency in the 2D (ω_t , ω_τ) spectrum measured at the same experimental conditions. Therefore, this approach was applied only when a single peak along the ω_t frequency was observed in the 2DIR spectra measured at the same experimental conditions.²⁷ Then, the cross-peak amplitude was determined for each ω_t absolute-value spectrum by integrating the peak in the vicinity of its maximum (at the level of ca. 70% from the maximum) and subtracting the integrated and normalized background. The resulting peak amplitudes were plotted as a function of the waiting time, T.

2.2. Sample Preparation and Linear Spectra. Samples contained 150 mM leucine- d_{10} -Boc (Leu- d_{10} -Boc) (CDN Isotopes Co.) in CHCl₃, the structure and the spectrum of which are presented in Figures 1A and 2, respectively, 35 mM of leucine- d_{10} -methyl ester hydrochloride (Leu- d_{10} -OMe)⁵⁵ in isopropanol (Figure 1B), or leucine- d_{10} amino acid in water (Figure 1C). The samples were held in the optical cell with CaF₂ windows of 50 or 10 μ m path length when dissolved in organic solvents and water, respectively. The linear IR spectra were measured using a Nexus 670 FTIR spectrometer.

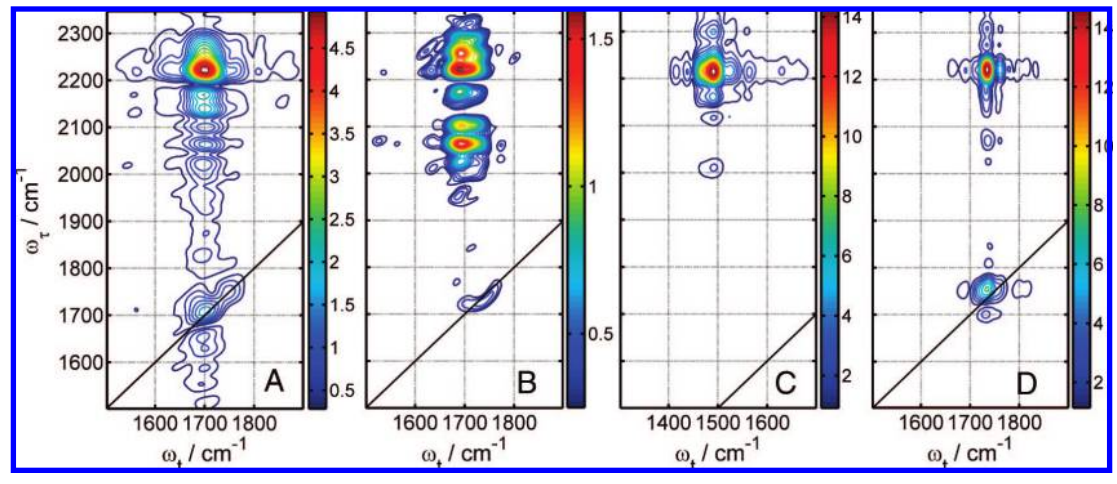


Figure 3. 2DIR spectra collected for Leu- d_{10} -Boc: (A) T=300 fs, (B) T=3 ps, both for the CD/CO cross peaks; (C) T=300 fs, focusing on the CD/Am–II cross peaks. (D) 2DIR spectrum of Leu- d_{10} -OMe collected at T=300 fs focusing on the CD/CO cross peaks. The k_1 and k_2 pulse spectra were centered at 2220 cm⁻¹ for A, C, and D graphs and at 2100 cm⁻¹ for graph B.

3. Results and Discussion

3.1. Coupling between CD and Carbonyl Stretching Modes. 2DIR measurements were performed on Leu- d_{10} -Boc dissolved in chloroform, focusing on the cross peak between the carbonyl and CD stretching modes. For these measurements the k_1 and k_2 pulse spectra were centered at ca. 2220 cm⁻¹, exciting the CD transitions, and the k_3 and LO pulse spectra were centered at 1712 cm⁻¹, accessing the carbonyl stretching modes. The 2DIR spectrum recorded at T = 300 fs (Figure 3A) shows the cross peaks between the mode at ca. 1700 cm⁻¹ and several C–D modes, as well as two strongly suppressed diagonal peaks at ca. 1700 and 1745 cm⁻¹. The dominant feature in the spectrum ω_t , ω_τ) = (1700, 2220 cm⁻¹), comes from interaction of the strongest CD transition and the main band of the carbonyl stretching modes.

The diagonal peaks at 1712 and 1745 cm⁻¹, although strongly suppressed, are also apparent because of nonzero light intensity of the k_1 , k_2 pulses at 1745 cm⁻¹ and even at 1700 cm⁻¹. The fit of the carbonyl stretching band around 1700 cm⁻¹ using Gaussian functions reveals two transitions at 1711 and 1751 cm⁻¹, with a ratio of amplitudes of 21:1 and respective widths (fwhm) of 37 and 43 cm⁻¹; these peaks are clearly resolved in the diagonal part of the 2DIR spectrum in Figure 3A. These transitions are attributed to the carbonyl stretching and Am-I modes, which are expected to be partially mixed and delocalized. 1,56 Nevertheless, the 2DIR spectrum clearly demonstrates that there is a substantial direct coupling between the carbonyl modes and several CD modes. Because the two carbonyl transitions are not resolved in the cross peaks (Figure 3A), we investigated CD/CO coupling in the Leu- d_{10} -OMe compound, which features a single carbonyl stretching mode. The 2DIR spectrum of Leu d_{10} -OMe dissolved in isopropanol is shown in Figure 3D. It shows several strong CD/CO cross peaks and severely suppressed diagonal CO peak at ca. (1740, 1740 cm⁻¹). Note that the linear spectrum of the CD stretching modes of Leu- d_{10} -OMe is very similar to that of Leu- d_{10} -Boc.

The Leu- d_{10} -Boc compound features a single Am-II mode at 1497 cm⁻¹ that also can serve as a structural label (Figure 2). The 2DIR spectrum measured at T = 300 fs (Figure 3C) shows the cross peaks between CD and Am-II modes in Leu- d_{10} -Boc. The cross peak among the Am-II mode and the strongest CD transition at 2220 cm⁻¹ dominates the spectrum. To characterize the CD transitions in these compounds, we used the RA 2DIR method and studied energy transport patterns,

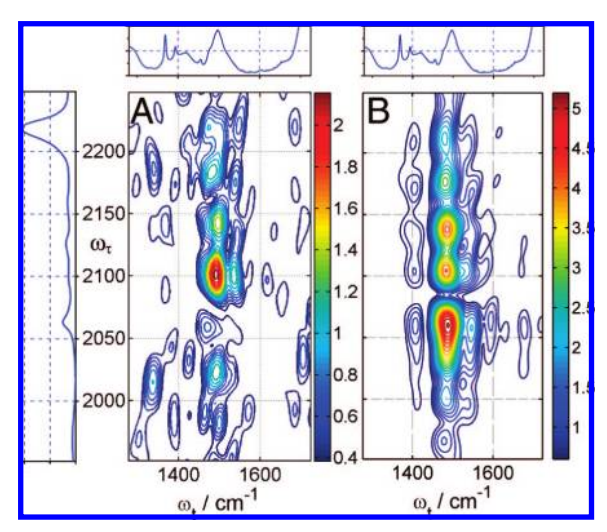


Figure 4. 2DIR spectra of Leu- d_{10} -Boc focusing on CD/Am-II cross peaks collected at T=200 fs (A) and T=3 ps (B). The k_1 and k_2 pulse spectra were centered at 2100 cm $^{-1}$.

focusing on the CD/Am–II and CD/CO multiple cross peaks in Leu- d_{10} -Boc and Leu- d_{10} -OMe, respectively.

Figure 4 shows examples of 2DIR spectra of Leu- d_{10} -Boc collected at the waiting times of 0.2 and 3 ps, which focus on the CD/Am–II cross peaks. The 2DIR spectrum at a small waiting time, T=0.2 ps, is dominated by the peak at (1497, 2100 cm⁻¹) indicating substantial anharmonic coupling among these modes (Figure 4A), and suggesting spatial closeness of the respective groups. Other cross-peaks in Figure 4A are weaker, rising barely above the noise level. Note that several factors affect the cross-peak amplitude, such as the anharmonic mode coupling strength and the efficiencies of photoexcitation of the two modes forming the cross peak.²³ The latter depends on the transition dipole values (extinction coefficients) for the two modes and the IR intensity at the frequencies of the modes absorption.

The 2DIR spectrum collected at the waiting time of 3 ps (Figure 4B) shows CD/Am–II cross peaks at (1497, 2062 cm⁻¹), (1497, 2100 cm⁻¹), (1497, 2145 cm⁻¹), (1497, 2180 cm⁻¹), and (1497, 2220 cm⁻¹), which occur due to a relaxation-assisted mechanism (vide infra). Similar to the direct-coupling cross peaks, the relaxation-assisted cross peaks depend on the efficiencies of modes photoexcitation. The peak at (1497, 2062

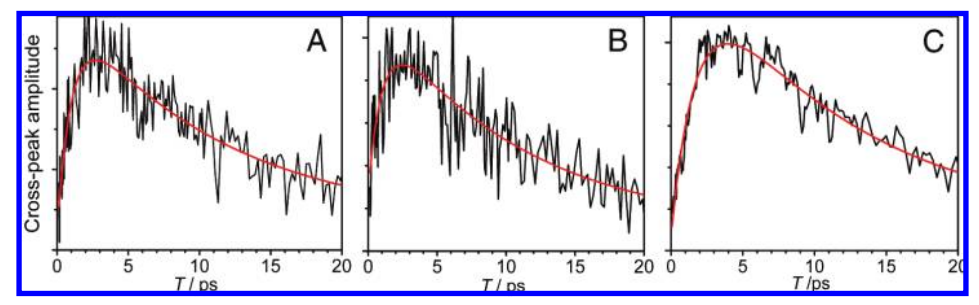


Figure 5. The waiting time, T, evolution of the cross-peak amplitudes for several CD/Am-II cross peaks: (A) 2062 cm⁻¹/Am-II, (B) 2220 cm⁻¹/Am-II, and (C) (2090-2195 cm⁻¹)/Am-II; the latter includes several smaller CD peaks. The red smooth lines are the fits with a twoexponential function used to determine peak positions.

TABLE 1: Arrival Times (T_{max}) and Amplification Factors (γ) Measured for Different Mode Pairs in Leu- d_{10} -Boc and Leu- d_{10} -OMe.^a

	Leu-d ₁₀ -Boc: CD/Am-II						Leu- d_{10} -OMe: CD/CO		
cross peaks	2062/ Am-II	2100/ Am-II	2145/ Am-II	2180/ Am-II	2220/ Am-II	2090-2195/ Am-II	2062/CO	2090-2195/CO	2220/CO
T_{max} , ps amplification factor, γ	$3 \pm 0.4 \\ 4 \pm 0.7$	2.0 ± 0.6 2.3 ± 0.8	2.8 ± 0.7 2.4 ± 0.7	2.5 ± 0.6 2.7 ± 0.5	4.0 ± 0.3 5 ± 0.5	2.5 ± 0.4 2.8 ± 0.5	$3.5 \pm 0.5 5 \pm 0.5$	3.1 ± 0.5 4.0 ± 0.5	4.2 ± 0.3 6.0 ± 1.2

^a The 2220/Am-II and 2220/CO cross peaks were measured with a k₁, k₂ pulse spectra at 2220 cm⁻¹, whereas for all other cross peaks the k_1 , k_2 pulse spectra were at 2100 cm⁻¹.

cm⁻¹) dominates the spectrum because of a relatively large extinction coefficient of the peak at 2062 cm⁻¹. Large extinction coefficient of the peak at 2220 cm⁻¹ makes the cross peak at (1497, 2220 cm⁻¹) visible in this experiment, despite very small light intensity at 2220 cm⁻¹. Although there are many experimental parameters that affect relative amplitudes of different cross peaks, including the differences in phase-matching conditions, which are difficult to control accurately, the changes in the amplitude of individual cross peaks as a function of the waiting time are easily measurable (see Experimental Methods) and informative.²⁷

3.2. Energy Transport Patterns Studied by the RA 2DIR **Method.** Figure 5 shows the waiting-time dependence of the CD/AM-II cross-peak amplitudes in Leu- d_{10} -Boc. For each measurement the spectra of the IR pulses were tuned close to the frequencies of the modes forming the cross peak, and the (τ, T) 2D data sets were acquired. Note that the (ω_{τ}, T) spectra obtained by the Fourier transformation along the τ direction of the (τ, T) data sets are similar to the projection of the 2DIR spectrum measured at the same waiting time, T, onto the ω_{τ} axis. Because there is only one peak seen in the 2DIR (τ, t) spectrum with ω_{τ} equal to 2220 cm⁻¹, the peak at the same frequency in the (ω_{τ}, T) data reports on the CD/Am-II cross peak. The amplitude of the 2220/Am-II cross peak as a function of T is shown in Figure 5C. To determine the maximum, the data were fitted using a two-exponential function (Figure 5). The cross peak grows with T and reaches maximum at the delay time T_{max} , (e.g., T_{max} value for the 2220/Am-II cross peak is 4.0 ± 0.3 ps), which is referred to as the (energy) arrival time. The maximum cross-peak amplitude is achieved when the vibrational energy from the photoexcited CD modes reaches, via energy transport and dissipation process, the Am-II mode site, exciting lower-frequency modes there, some of which are strongly coupled to the Am-II mode. 27 The amplification factor, γ , which is the ratio of the cross peak amplitude at the maximum to the amplitude at T = 0, 38 was also determined from the fitting curve. Figures 5A and 5C show the cross peak evolution of the peaks at 2062 and 2220 cm⁻¹, respectively.

To characterize the weaker CD transitions of Leu- d_{10} , the k_1 and k_2 laser pulses were centered at 2100 cm⁻¹; such pulses are optimal to excite the CD mode between 2062 and 2150 cm⁻¹ and have limited intensity at 2220 cm⁻¹, thus suppressing the strongest cross peak at $\omega_{\tau} = 2220 \text{ cm}^{-1}$. As before, the k_3 and LO pulses were centered at 1500 cm⁻¹ (Am–II). However, these cross peaks were much weaker than the cross peak at 2220 cm⁻¹, compromising the accuracy of the measurements of individual peaks. A combined curve was generated by integrating all cross peaks in the ω_{τ} range from 2090 to 2195 cm⁻¹ (Figure 5B). In addition to 2DIR (τ, T) measurements, a series of 2DIR spectra were collected at several characteristic waiting times to confirm the relative changes of the cross peak amplitudes (Figure 4 shows two examples). The amplification factors and arrival times for Leu- d_{10} -Boc and Leu- d_{10} -OMe are presented in Table 1 along with the central frequencies of the k_1 and k_2 pulses.

The observed differences in the arrival times measured for the CD/Am-II and CD/Am-I cross peaks for different CD transitions in Leu- d_{10} -Boc and Leu- d_{10} -OMe (Table 1) suggest that the 10 CD transitions are not fully delocalized over the whole side chain but form several groups with substantial mode delocalization within the group and relatively weak coupling between the modes of different groups.

Assuming monotonic dependence of the arrival time on the intermode distance, the RA 2DIR data alone could be used for assigning different CD peaks in the absorption spectrum. However, because there are very limited data demonstrating the monotonic dependence of T_{max} of R, in this work we used DFT calculations to aid the mode assignment and then tested how well the arrival time, T_{max} , correlates with the intermode distance,

3.3. Assignment of the CD Transitions in Leu- d_{10} Using **DFT Calculations.** Density functional theory (DFT) calculations, combined with the linear and 2D infrared experimental spectral data, permit deeper understanding of the origin of the CD transitions in the Leu- d_{10} compounds. Harmonic DFT calculations were performed on the Leu- d_{10} side chain fragment and the Leu- d_{10} amino acid using Gaussian-03d software (Gaussian Inc.) with the hybrid B3LYP functional and the 3–21G basis set (Figure 6A inset). The harmonic DFT analysis predicts that the splitting of the stretching modes in CD₂ and CD₃ moieties into symmetric and antisymmetric stretching

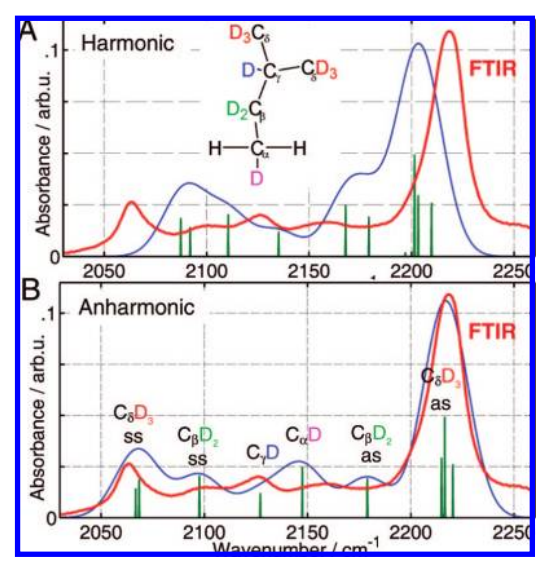


Figure 6. DFT harmonic (A) and anharmonic (B) modeling of the Leu- d_{10} side chain C-D absorption spectrum. The computed frequencies are shown by green bars; the blue line was obtained by introducing a broadening with Gaussian distribution function with 15 cm⁻¹ width. No scaling was used for the anharmonic frequencies, and the harmonic frequencies were scaled down by 4.8%. The FTIR spectrum of Leu- d_{10} -Boc in chloroform (thick red line) is shown on both panels for comparison.

modes amounts at 80 and 120 cm⁻¹, respectively, with the antisymmetric modes having higher frequencies. Note that there are two antisymmetric stretches for the CD₃ groups, which are almost degenerate on the harmonic level of calculations with the splitting of less than 1 cm $^{-1}$. The side group of Leu- d_{10} has two CD₃, one CD₂, and one CD moieties. Different splittings in the CD₃ and CD₂ groups of Leu-d₁₀ result in the stretching modes that are largely localized on the respective CD₃ and CD₂ groups. On the contrary, the states of the two $C_{\delta}D_3$ groups of Leu- d_{10} have very similar frequencies, which lead to, at least partial, delocalization of the respective vibrational wave functions over the two $C_\delta D_3$ groups. The harmonic DFT analysis, however, fails to reproduce important features of the experimental FTIR spectrum of Leu- d_{10} , most notably the total span of the C-D "band" (Figure 1B). The total span predicted by the harmonic DFT modeling with B3LYP functional is ca. 33 cm⁻¹ smaller than that observed experimentally (ca. 155 cm⁻¹).

DFT calculations of anharmonic frequencies implemented in Gaussian-03d via the perturbative approach⁵⁷ are extremely timeconsuming and were performed only for the Leu- d_{10} fragment (Figure 6A inset). The computed anharmonic spectrum shows very impressive agreement with the experimental spectrum (Figure 6B), indicating that the modeling is trustworthy. The modeling shows that the CD modes of Leu- d_{10} can be divided into several largely independent groups, so that the modes in a group are mostly delocalized on the atoms included in the group. The two strongest transitions in the linear spectrum are due to the group that includes two $C_{\delta}D_3$ moieties; the peaks at 2060 and 2218 cm⁻¹ encompass two symmetric stretching and four antisymmetric stretching transitions, respectively. The modes of the $C_{\beta}D_2$ moiety form another group with just two transitions: symmetric stretch at 2098 cm⁻¹ and antisymmetric stretch at 2179 cm⁻¹, which match two weak peaks in the FTIR spectrum. The two remaining C-D groups, $C_{\alpha}D$ and $C_{\nu}D$, are spatially separated and experience different environment, which likely prevents efficient mixing of their CD stretching modes. The $C_{\nu}D$ frequency (2127 cm⁻¹) falls between the $C_{\beta}D_2$ transitions, filling the central area of the C-D band of the Leu- d_{10} spectrum. The position of the $C_{\alpha}D$ transition is less certain, as the charge distribution on the backbone is affected by the protonation equilibria at the amino and carboxylic acid sites, which were not included into the computations. Moreover, the transition dipole of the $C_{\alpha}D$ transition is expected to be small, which makes it difficult to assign this mode in the experimental spectrum. Although the calculated $C_{\alpha}D$ frequency does not strongly contradict with the experimental spectrum, accurate assignment of the $C_{\alpha}D$ stretching mode to a specific peak in the linear spectrum was not done in this work.

3.4. Anisotropy and Lifetime Measurements. The anisotropy measurements were performed on the CD/Am-II cross peaks to test if the angular relations between Am-II and CD modes can be detected. Only a small difference in the cross peak amplitudes has been observed for parallel (zzzz) and perpendicular (zzxx) polarization conditions for the peaks at 2220/Am-II and 2062/Am-II, resulting in anisotropy values of 0.02 and 0.03, respectively. The anisotropy data support the assignment of the CD transitions at 2220 and 2062 cm⁻¹ to the multiple transitions of the two $C_{\delta}D_3$ groups, which should result in severely reduced cross-peak anisotropy values due to complex peak content.58,59 Structural inhomogeneity may contribute to the reduction of the cross-peak anisotropy as well. Anisotropy measurements for the cross peaks involving weaker CD transitions, whereas bearing a larger noise level showed anisotropy values smaller than 0.04. The lifetime of the strongest CD mode at 2220 cm⁻¹ is 1.3 ± 0.05 ps, which is much smaller than the lifetime of a single CD mode in deuterated haloforms in benzene and acetone (ca. 12 ps).60

Because of the small values of anisotropy for the cross peaks involving CD modes, all measurements were performed using parallel polarization conditions. The corrections caused by molecular rotation, which is, based on the molecular volume, expected to be ca. 50 ps, to the experimentally determined characteristic times are well within the error bars given for the respective values.

3.5. Correlation of the Arrival Time with the Intermode **Distance.** Using the mode assignment summarized in Figure 6 it is possible to test whether the arrival times and amplification coefficients correlate with the intermode distance. The distance between various CD modes in Leu-d₁₀-Boc and the Am-II mode, which is mostly localized at the C-N bond, is approximately equal to the number of bonds separating the respective CD bond from the C-N bond. For example, the modes associated with the $C_{\delta}D_3$ groups (2220 and 2062 cm⁻¹) are four bonds apart from the C-N bond; the modes associated with $C_{\alpha}D$, $C_{\beta}D_2$, and $C_{\gamma}D$ groups (Figure 6) are separated from the C-N bond by one, two, and three bonds, respectively. Figure 7 shows the dependence of $T_{\rm max}$ and γ on the intermode distance expressed as the number of separating bonds. Both $T_{\rm max}$ and γ correlate monotonically with the distance. For example, both T_{max} and γ for the $C_{\delta}D_3$ groups are larger than those for the $C_{\beta}D_2$ group. The cross peak at 2145/Am–II is expected to have contributions from the $C_{\alpha}D$ and $C_{\nu}D$ modes, which are difficult to separate. Assuming that the contribution of the $C_{\nu}D$ mode is dominant at 2145 cm⁻¹, the data for this cross peak are plotted at the intermode distance of three, which places the arrival time right on the monotonic dependence while the amplification coefficient falls off the monotonic trend. The data suggest that there is a significant contribution of the $C_{\alpha}D$ mode at 2145 cm⁻¹, which, due to its closeness to the Am-II, is expected to feature small (if any) cross peak amplification and a somewhat weak dependence of the cross-peak amplitude from the waiting time,

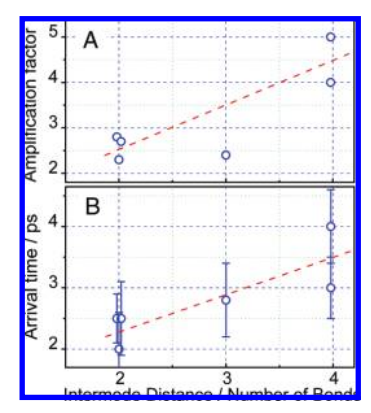


Figure 7. Amplification factors (A) and arrival times (B) measured for different CD/Am-II cross peaks in Leu- d_{10} -Boc. The red dashed lines serve as a guide to the eye.

T (at least for small values of T). A relatively "flat" contribution from the $C_{\alpha}D$ mode to the T-dependence would significantly decrease the apparent amplification coefficient, but only minimally affect the measured arrival time, which then mostly reflects the $C_{\gamma}D$ mode. Assuming that the amplification coefficient for the $C_{\gamma}D/Am-II$ cross peak is ca. 3.5, as predicted by the linear interpolation in Figure 7A, one can estimate the contribution of the $C_{\alpha}D$ mode to the 2145/Am-II cross-peak to be 80% from that of the $C_{\gamma}D$ mode. Note that the averaging window along ω_{τ} used to generate the data set for the 2145/Am-II cross-peak was 30 cm⁻¹ wide.

Despite the qualitative nature of the discussion for the 2145/Am–II cross peak, the whole data set shown in Figure 7 demonstrates a solid correlation of $T_{\rm max}$ and γ with the intermode distance supporting strongly the mode assignment made using DFT modeling.

3.6. Applicability of the C-D Label for Structural Measurements in Proteins. All CD stretching transitions of Leu d_{10} side chain broaden severely when placed in D_2O solvent. Due to the large width of the transitions, the groups exposed to D₂O will not have significant contributions in the 2DIR measurements. In addition, the optical density of the D₂O absorption at 2220 cm⁻¹ in a 25 μ m thick sample cell was only ca. 0.45, which is still practical for 2DIR measurements.³⁴ Therefore, only the Leu- d_{10} amino acids buried in the hydrophobic environment having narrow transitions with large extinction coefficients will be exclusively seen in 2DIR measurements in D_2O . The comparison of the Leu- d_{10} spectra in H₂O and D₂O shows that the broadening in D₂O is not due to the effect of polarity, as in the case reported for the SH stretching mode by Hamm and co-workers,36 but rather the influence of the OD transitions of D_2O on the CD modes in Leu- d_{10} . It is thus expected that the CD stretching transitions of Leu- d_{10} side chains will not only serve as convenient structural labels if placed in the hydrophobic core of a protein but will also report on the level of hydration in a particular site of the protein. Other amino acids with deuterated side chains can also provide convenient IR labels that are expected to be useful for structural measurements in proteins.

4. Summary

In summary, we have investigated the use of CD stretching transitions of the deuterated amino acid Leu- d_{10} as probes for structural via 2DIR spectroscopy. The assignment of the CD peaks of the linear absorption spectrum is performed by a combination of the DFT anharmonic calculations and the RA 2DIR measurements. A correlation is found between the arrival

time, amplification factor, and the intermode distance. Such correlation permits using multiple CD transition of the same side chain as correlated structural reporters. The 5-fold amplification found for the 2220 cm⁻¹ mode and Am-I or Am-II cross-peaks is important for enhancing the desired features in 2DIR spectra. The C-D label is expected to be very useful for structural measurements in proteins, especially when the label is surrounded by a hydrophobic environment.

Acknowledgment. The authors are thankful to the Tulane University Center for Computational Sciences and Louisiana Optical Network Initiative Institute for providing computational resources and to Mrs. Natalia Rubtsova for the help with the synthesis. Support is gratefully acknowledged from the NSF, CHE-0750415 to I.V.R., and MCB-0346967 to F.E.R.

References and Notes

- Hamm, P.; Lim, M.; Hochstrasser, R. M. J. Phys. Chem. B 1998, 102, 6123.
 - (2) Hochstrasser, R. M Proc. Natl. Acad. Sci. U.S.A. 2007, 104, 14190.
- (3) Mukamel, S. Principles of nonlinear spectroscopy; Oxford University Press: New York, 1995.
- (4) Ding, F.; Fulmer, E. C.; Zanni, M. T. In *Femtosecond 3D IR Spectroscopy*; Springer Series in Chemical Physics (Ultrafast Phenomena XV); Corkum, P., Jonas, D. M., Miller, R. J. D., Weiner, A. M. Eds.; Springer: Berlin, Heidelberg, New York, 2007; Vol. 88, p 404.
 - (5) Volkov, V.; Hamm, P. Biophys. J. 2004, 87, 4213.
- (6) Shim, S.-H.; Strasfeld, D. B.; Ling, Y. L.; Zanni, M. T. Proc. Natl. Acad. Sci. U.S.A. 2007, 104, 14197.
- (7) Demirdoeven, N.; Cheatum, C. M.; Chung, H. S.; Khalil, M.; Knoester, J.; Tokmakoff, A. *J. Am. Chem. Soc.* **2004**, *126*, 7981.
- (8) Backus, E. H. G.; Nguyen, P. H.; Botan, V.; Pfister, R.; Moretto, A.; Crisma, M.; Toniolo, C.; Stock, G.; Hamm, P. J. Phys. Chem. B 2008, 112, 9091.
- (9) Olano, C.; Helbing, J.; Kozinski, M.; Sander, W.; Hamm, P. *Nature* **2006**, *444*, 469.
 - (10) Zheng, J.; Fayer, M. D. J. Phys. Chem. B 2008, 112, 10221.
- (11) Cahoon, J. F.; Sawyer, K. R.; Schlegel, J. P.; Harris, C. B. Science **2008**, *319*, 1820.
 - (12) Cho, M. Chem. Rev. 2008, 108, 1331.
- (13) Kim, Y. S.; Hochstrasser, R. M. Proc. Natl. Acad. Sci. U.S.A. 2005, 102, 11185.
- (14) Asbury, J. B.; Steinel, T.; Fayer, M. D. J. Phys. Chem. B 2004, 108, 6544.
- (15) Kraemer, D.; Cowan, M. L.; Paarmann, A.; Huse, N.; Nibbering, E. T. J.; Elsaesser, T.; Miller, R. J. D. *Proc. Natl. Acad. Sci. U.S.A.* **2008**, *105*, 437.
- (16) Yeremenko, S.; Pshenichnikov, M. S.; Wiersma, D. A. Phys. Rev. A 2006, 73, 021804.
- (17) Bredenbeck, J.; Helbing, J.; Sieg, A.; Schrader, T.; Zinth, W.; Renner, C.; Behrendt, R.; Moroder, L.; Wachtveit, J.; Hamm, P. *Proc. Natl. Acad. Sci. U.S.A.* **2003**, *100*, 6452.
- (18) Chung, H. S.; Ganim, Z.; Jones, K. C.; Tokmakoff, A. *Proc. Natl. Acad. Sci. U.S.A.* **2007**, *104* (36), 14237.
- (19) Bredenbeck, J.; Helbing, J.; Nienhaus, K.; Nienhaus, G. U.; Hamm, P. *Proc. Natl. Acad. Sci. U.S.A.* **2007**, *104*, 14243.
- (20) Hamm, P.; Helbing, J.; Bredenbeck, J. Annu. Rev. Phys. Chem. 2008, 59, 291.
- (21) Strasfeld, D. B.; Ling, Y. L.; Shim, S.-H.; Zanni, M. T. J. Am. Chem. Soc. 2008, 130, 6698.
- (22) Kim, Y. S.; Liu, L. A. H. P.; Hochstrasser, R. M. *Proc. Natl. Acad. Sci. U.S.A.* **2008**, *105*, 7720.
- (23) Hamm, P.; Hochstrasser, R. M. Structure and Dynamics of Proteins and Peptides: Femtosecond Two-Dimensional Infrared Spectroscopy In *Ultrafast Infrared and Raman Spectroscopy*; Fayer, M. D., Ed.; Marcel Dekker Inc.: New York, 2000; p 273.
- (24) Rubtsov, I. V.; Wang, J.; Hochstrasser, R. M. Proc. Natl. Acad. Sci. U.S.A. 2003, 100, 5601.
- (25) Rubtsov, I. V.; Kumar, K.; Hochstrasser, R. M. Chem. Phys. Lett. 2005, 402, 439.
- (26) Kurochkin, D. V.; Naraharisetty, S. R. G.; Rubtsov, I. V. J. Phys. Chem. A 2005, 109, 10799.
- (27) Kurochkin, D. V.; Naraharisetty, S. R. G.; Rubtsov, I. V *Proc. Natl. Acad. Sci. U.S.A.* **2007**, *104*, 14209.
- (28) Ernst, R. R.; Bodenhausen, G.; Wokaun, A. *Principles of Nuclear Magnetic Resonance in One and Two Dimensions*; Oxford University Press: New York, 1987.

- (29) Fang, C.; Wang, J.; Charnley, A. K.; Barber-Armstrong, W.; Smith, A. B.; Decatur, S. M.; Hochstrasser, R. M. *Chem. Phys. Lett.* **2003**, *382*, 586.
- (30) Kumar, K.; Sinks, L. E.; Wang, J.; Kim, Y. S.; Hochstrasser, R. M. Chem. Phys. Lett. **2006**, 432, 122.
- (31) Mukherjee, P.; Kass, I.; Arkin, I.; Zanni, M. T. *Proc. Natl. Acad. Sci. U.S.A.* **2006**, *103*, 3528.
 - (32) Fang, C.; Hochstrasser, R. M. J. Phys. Chem. B 2005, 109, 18652.
- (33) Naraharisetty, S. R. G.; Kurochkin, D. V.; Rubtsov, I. V. Chem. Phys. Lett. 2007, 437, 262.
- (34) Fang, C.; Baumann, J. D.; Das, K.; Remorino, A.; Arnold, E.; Hochstrasser, R. M. *Proc. Natl. Acad. Sci. U.S.A.* **2008**, *105*, 1472.
- (35) Lindquist, B. A.; Haws, R. T.; Corcelli, S. A. J. Phys. Chem. B 2008, 112, 13991.
- (36) Kozinski, M.; Garrett-Roe, S.; Hamm, P. J. Phys. Chem. B 2008, 112, 7645.
- (37) Rubtsov, I. V.; Naraharisetty, S. G.; Keating, C.; McClure, B. A.; Rack, J. J.; Kasyanenko, V. M., *Relaxation-assisted Dual-frequency Two-dimensional Infrared Spectroscopy: Measuring Distances and Bond Connectivity*; Springer Series in Chemical Physics, Ultrafast Phenomena XVI; Springer: Berlin, Heidelberg, New York, 2009.
- (38) Naraharisetty, S. R.G.; Kasyanenko, V. M.; Rubtsov, I. V. *J. Chem. Phys.* **2008**, *128*, 104502/1.
- (39) Fang, C.; Senes, A.; Cristian, L.; DeGrado, W. F.; Hochstrasser, R. M. *Proc. Natl. Acad. Sci. U.S.A.* **2006**, *103*, 16740.
- (40) Chin, J. K.; Jimenez, R.; Romesberg, F. E. J. Am. Chem. Soc. 2002, 124, 1846.
- (41) Chin, J. K.; Jimenez, R.; Romesberg, F. E. J. Am. Chem. Soc. 2001, 123, 2426.
- (42) Cremeens, M. E.; Fujisaki, H.; Zhang, Y.; Zimmermann, J.; Sagle, L. B.; Matsuda, S.; Dawson, P. E.; Straub, J. E.; Romesberg, F. E. *J. Am. Chem. Soc.* **2006**, *128*, 6028.
- (43) Sagle, L. B.; Zimmermann, J.; Dawson, P. E.; Romesberg, F. E. J. Am. Chem. Soc. 2004, 126, 3384.

- (44) Sagle, L. B.; Zimmermann, J.; Dawson, P. E.; Romesberg, F. E. J. Am. Chem. Soc. **2006**, *128*, 14232.
- (45) Sagle, L. B.; Zimmermann, J.; Matsuda, S.; Dawson, P. E.; Romesberg, F. E. *J. Am. Chem. Soc.* **2006**, *128*, 7909.
- (46) Weinkam, P.; Zimmermann, J.; Sagle, L. B.; Matsuda, S.; Dawson, P. E.; Wolynes, P. G.; Romesberg, F. E. *Biochem.* **2008**, *47*, 13470.
- (47) Thielges, M. C.; Case, D. A.; Romesberg, F. E. J. Am. Chem. Soc. 2008
- (48) Torok, Z.; Szalontai, B.; Joo, F.; Wistrom, C. A.; Vigh, L. *Biochem. Biophys. Res. Com.* **1993**, 92, 518.
- (49) Fawcett, W. R.; Liu, G.; Kessler, T. E. J. Phys. Chem. 1993, 97, 9293
- (50) Sibert, E. L.; Reinhardt, W. P.; Hynes, J. T. J. Chem. Phys. 1984, 81, 1115.
- (51) Kinnaman, C. S.; Cremees, M. E.; Romesberg, F. E.; Corcelli, S. C. J. Am. Chem. Soc. **2006**, 128, 13335.
- (52) Ha, J.-H.; Kim, Y. S.; Hochstrasser, R. M. J. Chem. Phys. 2006, 124, 064508/1.
- (53) Stenger, J.; Madsen, D.; Hamm, P.; Nibbering, E. T. J.; Elsaesser, T. J. Phys. Chem. A 2002, 106, 2341.
- (54) Kurochkin, D. V.; Naraharisetty, S. R. G.; Rubtsov, I. V. *Relaxation-Assisted 2D IR Using Weak Vibrational Modes*; 15th International Conference on Ultrafast Phenomena, Pacific Grove, CA, 2006.
 - (55) Brenner, M.; Huber, W. Helv. Chim. Acta 1953, 36, 1109.
 - (56) Hamm, P.; Woutersen, S. Bul. Chem. Soc. Japan 2002, 75, 985.
 - (57) Barone, V. J. Chem. Phys. 2005, 122, 014108.
 - (58) Hochstrasser, R. M. Chem. Phys. 2001, 266, 273.
- (59) Golonzka, O.; Khalil, M.; Demirdoven, N.; Tokmakoff, A. *J. Chem. Phys.* **2001**, *115*, 10814.
- (60) Gundogdu, K.; Nydegger, M. W.; Bandaria, J. N.; Hill, S. E.; Cheatum, C. M J. Chem. Phys. **2006**, 125, 174503/1.

JP8112446